

Spatial-temporal variation characteristics of air pollution and apportionment of contributions by different sources in Shanxi province of China

Xiaoxuan Bai ^{a,b,*}, Hezhong Tian ^{a,b,*}, Xiangyang Liu ^{a,b}, Bobo Wu ^{a,b}, Shuhan Liu ^{a,b}, Yan Hao ^{a,b}, Lining Luo ^{a,b}, Wei Liu ^{a,b}, Shuang Zhao ^{a,b}, Shumin Lin ^{a,b}, Jiming Hao ^c, Zhihui Guo ^{a,b}, Yunqian Lv ^{a,b}

^a State Key Joint Laboratory of Environmental Simulation & Pollution Control, School of Environment, Beijing Normal University, Beijing, 100875, China

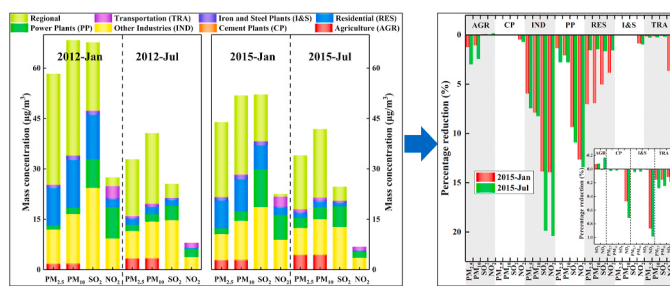
^b Center for Atmospheric Environmental Studies, Beijing Normal University, Beijing, 100875, China

^c School of Environment, Tsinghua University, Beijing, 100084, China

HIGHLIGHTS

- The first overall estimation of air pollution evolution in Shanxi is presented.
- Spatial-temporal pollution characteristics are investigated by WRF-CAMx model.
- Heavy contaminated areas have shown negligible variations from 2012 to 2015.
- Industries, residential, and power plants are main local pollution contributors.
- Mitigation potential for each city varies each other and more effective in summer.

GRAPHICAL ABSTRACT



ARTICLE INFO

Keywords:
Primary air pollutants
WRF-CAMx model
Sectoral contribution
Mitigation potentials
Shanxi province of China
Prefecture-level city

ABSTRACT

With the implementation of the Air Pollution Prevention and Control Action Plan (APPACAP) since 2013, significant declines in pollutants concentrations have achieved in nationwide of China. However, as one of the major coal-production bases and intensive energy-consuming provinces in China, Shanxi has still been suffering from severe air quality problems in recent years. In this study, by combining a detailed bottom-up emission inventory and the weather research and forecasting (WRF) model/comprehensive air quality model with extensions (CAMx) model, the evolution of pollutant concentrations, source apportionment, and migration potentials from 2012 to 2015 in Shanxi are investigated. Estimated primary air pollutants emission declined significantly during 2012–2015. Compared with 2012, the simulated concentrations of PM_{2.5}, PM₁₀, SO₂ and NO₂ in January of 2015 are reduced by 24.7%, 24.1%, 23.0% and 18.0%, respectively. In contrast, heavy contaminated areas have shown negligible variations, which are highly concentrated in Taiyuan, Linfen, Jincheng, Changzhi, Lvliang, Yangquan and Jinzhong cities. In terms of contribution by source categories, the other industries and residential sources are identified as the most significant local contributors for PM_{2.5} and PM₁₀, while SO₂ and NO₂ are mainly emitted by other industries and power plants. Scenarios analysis of 50% emission

* Corresponding author. State Key Joint Laboratory of Environmental Simulation & Pollution Control, School of Environment, Beijing Normal University, Beijing 100875, China.

E-mail address: hztian@bnu.edu.cn (H. Tian).

mitigation suggests that the emission reduction measures are generally more effective in summer than in winter. Moreover, the mitigation potential for each city varies from each other. These results indicate that more appropriate seasonal-specific emission reduction measures in each prefecture-level city should be implemented to further improve regional air quality and thus better protect public health.

1. Introduction

The emissions of air pollutants have increased significantly driven by the rapid economic growth, urbanization, and population expansion all over the world, especially in China (HEI, 2019; WB, 2016; Zhang et al., 2012a). Moreover, long-term exposure to ambient fine particulate matter ($\leq 2.5 \mu\text{m}$ in aerodynamic diameter; PM_{2.5}) could pose an urgent threat to human health and even cause deaths (Anderson et al., 2012; Liu et al., 2018b; Lu et al., 2019; Valavanidis et al., 2008; Xu et al., 2013). Shanxi province, which is largely located in the basin between Lvliang Mountains and Taihang Mountains and represents one of the major coal-production bases and intensive energy-consuming provinces in mainland China, has been suffering from severe air pollution problems during the past years. In particular, six among the total eleven prefecture-level cities of Shanxi (Linfen, Taiyuan, Jincheng, Yangquan, Yuncheng and Jinzhong) were listed in the top twenty polluted cities of mainland China with severe air pollution in 2018. Thus, it is quite necessary to know well the air pollution status and major sensitive contributors in different cities of Shanxi province so as to further improve the regional air quality and protect public health.

To restrain the frequently occurrences of serious PM_{2.5} pollution in large areas of mainland China, the Chinese central government released the Air Pollution Prevention and Control Action Plan (APPCAP) in September 2013, which is aimed to mitigate severe PM pollution across China, especially in the most highlighted area of Beijing-Tianjin-Hebei (BTH) region. Meanwhile, the several surrounding provinces of BTH region, including Henan, Shandong and Shanxi province, are also requested to implement the APPCAP and issue their local action plans,

and consequently, air quality of the whole region has attained remarkable improvements during the past 5 years (Cai et al., 2017; Liu et al., 2016; Wang et al., 2017a; Zhao et al., 2017a; Zheng et al., 2018). As illustrated in Fig. S1, from 2013 to 2018, the average annual concentrations of PM_{2.5}, PM₁₀ and SO₂ in Shanxi Province are decreased by 29.5%, 10.1% and 50.0%, respectively, with a significant declined amplitude in 2015.

Shanxi Province, is located in northern China, and has jurisdiction over an area of 156700 km² and a household-registration population of 37.18 million. Its coal reserves are about 916.2 billion tons in 2016, accounting for 36.8% of the total coal resources in China (NBSC, 2017). Coal metallurgical machinery and several other pillar industries (like coal-fired power plants, iron & steel smelting, coal coking, etc.) which are featured with energy-intensive in Shanxi province, have caused a large number of particulate matters (PM₁₀, PM_{2.5}) and other gaseous pollutants (SO₂, NO_x, etc.) emitted into the atmosphere (Yan et al., 2016). Furthermore, the terrain of Shanxi is high in the north while low in the south. There are plateaus and mountains in the West (the Loess Plateau plateaus and Lvliang Mountains) and East (Taihang Mountains), and basin and valleys in the middle. The special narrow and long basin geography of Shanxi (shown in Fig. 1) leads to poor diffusion conditions, easily causing the accumulation of pollutants (Li et al., 2018). Moreover, several studies found that emissions in Shanxi contributed elevated air pollution for the neighboring BTH region through inter-province trans-boundary transportation. Wang et al. (2012) analyzed a heavy pollution episode over the southern Hebei using Community Multiscale Air Quality Model (CMAQ) modeling simulation, and their results indicated that more than 10% of the PM_{2.5} in southern Hebei area originated from

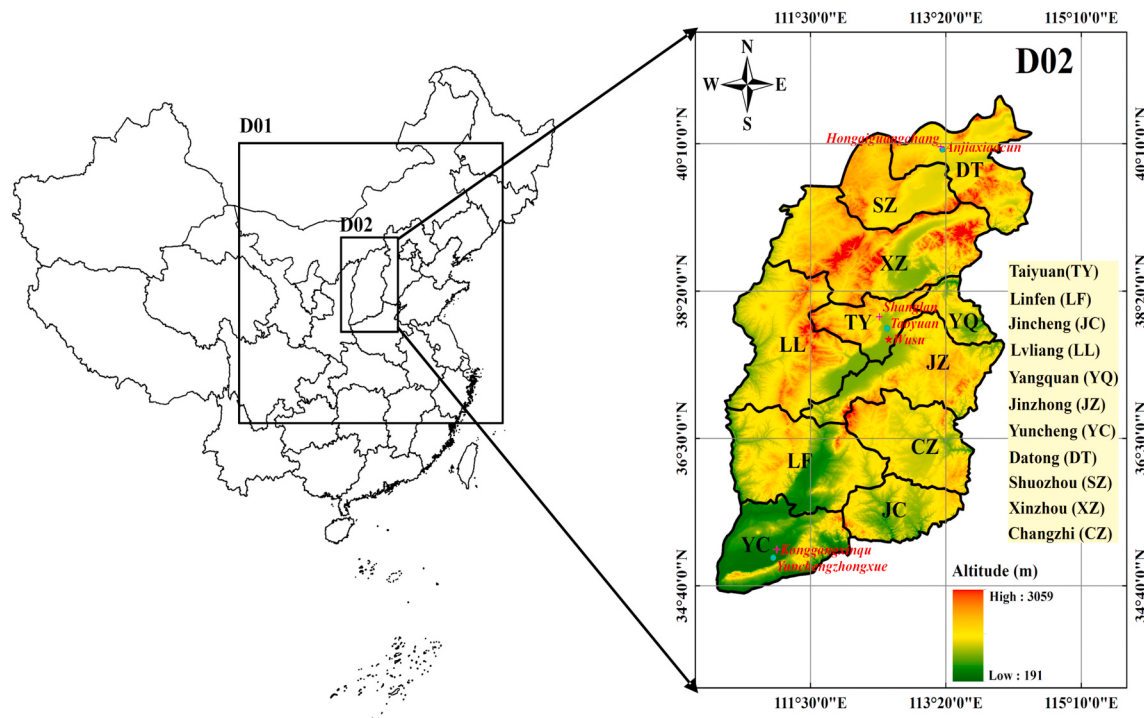


Fig. 1. CAMx modeling domains at a horizontal grid resolution of 27 km over Domain 1 and 9 km over Domain 2. Locations of meteorology (red star), urban pollutants concentration (blue dots) and rural pollutants concentration (purple cross) monitoring stations. (For interpretation of the references to colour in this figure legend, the reader is referred to the Web version of this article.)

the western neighboring Shanxi province. According to the results of Chang et al. (2019), the annual averaged contribution from Shanxi to the 13 cities in the BTH region is 1.2–5.5% for the year 2014.

In the past few decades, 3-D Air quality model has been increasingly applied to explore the temporal and spatial characteristics of hazardous air pollutants (HAPs), identify contributions by different sectors, and assess potentials of emission mitigation (Wang et al., 2017b). However, most of previous studies are focused on mainland China or the major polluted regions such as Beijing and Hebei in China. Wang et al. (2014) applied the MM5-CMAQ model to simulate the 2013 severe winter hazes in southern Hebei, and the source contributions of major source regions and sectors to PM_{2.5} concentrations in the three most polluted cities in southern Hebei are quantified by aiming at the understanding of the sources of severe haze pollution in this region. Ma et al. (2017) conducted standard and sensitivity simulations to quantitatively identify the contributions of coal combustion in different sectors to ambient PM_{2.5} in China by using the chemical transport model GEOS-Chem. Tan et al. (2017) simulated the air quality of Shanghai with WRF-CMAQ model at non-pollution and heavy pollution episodes in 2012, and investigated and quantified the uncertainties of meteorological and air quality model during multi-levels air pollution periods. Cheng et al. (2018) combined a detailed bottom-up emission inventory and the WRF-CMAQ model to quantify the contribution of changes in meteorological conditions, reduction of emissions from surrounding regions, and seven specific categories of local emission control measures to the PM_{2.5} changes in Beijing during 2013–2017. Bo et al. (2019) used the Comprehensive Air Quality Model with extensions (CAMx) to measure the corresponding environmental impacts from all civil airports in mainland China. However, till now, a dedicatedly study on investigating the temporal and spatial variations of air pollution characteristics across Shanxi province is still quite limited, which is of great significant for implementing regional joint air pollution control policies and improving air quality both in Shanxi and its surrounding provinces.

In this study, the spatial-temporal variation characteristics of air pollution from the year 2012–2015 across Shanxi province were simulated by applying the WRF-CAM_X model at the resolution of 9 × 9 km. Then, we evaluated the performance of the baseline simulation and examined the contributions of different sectors to several key criterion air pollutants (PM_{2.5}, PM₁₀, SO₂ and NO₂) across Shanxi by applying the Particulate Matter Source Apportionment Technology (PSAT) module embedded in the CAM_X model system. Finally, sensitivity analysis was conducted to quantify the mitigation potentials for each sector emissions in each prefecture-level cities.

2. Methodology and data sources

2.1. Modeling domain and episodes

As shown in Fig. 1, WRF and CAM_X simulations were performed over two nested domains: The central and eastern part of China with a grid resolution of 27 × 27 km (Domain 1) and the Shanxi provinces with a high-resolution grid resolution of 9 × 9 km (Domain 2), which centered at 37.75° N, 112.40° E on the Lambert Conformal. The projection was a Lambert projection with two true latitudes of 25° N and 47° N. The boundary conditions for Domain 2 was generated by Domain 1. The model simulations were conducted for the period of January and July in both the year 2012 and 2015, representing the typical seasons of winter and summer during a whole year.

All 11 prefecture-level cities of Shanxi province were investigated to better detail the spatial and temporal variations of pollution characteristics and regional source contributions in Shanxi Province. These 11 cities (see Fig. 1) were Taiyuan (TY), Linfen (LF), Jincheng (JC), Yangquan (YQ), Jinzhong (JZ), Yuncheng (YC), Lvliang (LL), Xinzhou (XZ), Changzhi (CZ), Shuozhou (SZ) and Datong (DT), respectively.

2.2. Model configurations and inputs

2.2.1. WRF-CAM_X model

WRF v3.7 (Skamarock et al., 2008) and CAMx 6.4 (ENVIRON, 2016) model systems were applied in this study. WRF model provided the meteorological conditions to drive the running of CAMx. CAMx with PSAT tool was applied to simulate air quality and apportion major sources of primary air pollutants. A spin-up period of 10 days was used to minimize the influence of the initial conditions.

For the WRF model, the US National Center for Environmental Prediction (NCEP) final operational global analysis dataset (<http://dss.ucar.edu/datasets/ds083.2>) was utilized to set the initial and boundary conditions. Moreover, the land use/cover and topographical data were established on the 30-s resolution default WRF input dataset. There were 30 sigma levels from the surface to 15 km for the WRF meteorological modeling. We chose the WSM3 microphysical schemes, the RRTM radiation scheme, the Kain-Fritsch cloud parameterization (Kain, 2004), the Yonsei PBL parameterization scheme (Pleim, 2006, 2007), and the Noah land-surface model for the model configurations (Pleim and Xiu, 1994; Xiu and Pleim, 2000).

For the CAMx model, the piecewise parabolic method (PPM) advection scheme was used for horizontal advection (Colella and Woodward, 1984). Gas-phase chemistry was simulated with the CB05 mechanism (Yarwood et al., 2005) with Euler Backwards Iterative (EBI) solver. Aerosol processes were modeled using the CF algorithm, which divided the size distribution into coarse and fine modes. Partitioning of inorganic aerosol constituents between gas and aerosol phases used the ISORROPIA thermodynamic module (Nenes et al., 1998). Besides, boundary condition for Domain 1 was generated from the MOZART4 (<https://www.acm.ucar.edu/wrf-chem/mozart.shtml>) global chemistry transport model (Wang et al., 2016). The vertical axis covered 14 sigma levels ranging from the surface to 15 km altitudes. Furthermore, particulate matter source apportionment technology (PSAT) was adopted to calculate apportionment among specific source categories of geographic regions.

2.2.2. Emission inventory data

In this study, the air pollutant multi-resolution emission inventory in China (MEIC) (<http://www.meicmodel.org/dataset-meic.html>) was used for the surrounding regions of Shanxi province. It should be noted that the MEIC for the year 2014 was used to represent 2015 emissions. The refined multi-resolution (9 km × 9 km) unit-based emission inventory for the years 2012 (Liu et al., 2018a) and 2015 established by Prof. Hezhong Tian's group in Beijing Normal University (BNU) was used as input for Shanxi province, of which the emissions of SO₂, NO_x, PM₁₀, PM_{2.5}, VOCs, CO, and NH₃ from varied source categories were estimated. The detailed methodologies and source data on developing emission inventory could be referred to our previous study (Liu et al., 2018a). Natural sources were not considered temporarily in this study because it was difficult to control by government (Wang et al., 2014). Furthermore, in order to better identify and explore the contributions on emissions and ambient concentrations of several key source categories, the initial input emission inventory of Shanxi was classified into seven main source categories, i.e. power plants (PP), cement plants (CP), iron and steel plants (I&S), residential use (RES), transportation (TRA), agriculture (AGR), and other industries (IND). In addition, the initial emission inventory was processed by the Sparse Matrix Operator Kernel Emissions (SMOKE) model for adapting the request of air quality modeling (Liu et al., 2018b, 2019).

2.2.3. Scenario design for sensitivity analysis

To quantify the potential for reducing several key criterion air pollutants (including PM_{2.5}, PM₁₀, SO₂, and NO₂) of Shanxi province, we set up 7 sensitivity simulations for Domain 2 to investigate the responses of concentration variations due to emission reductions in the study area based on 2015 baseline emission inventory. The description and details

of all scenarios are presented in Table S1. During the period of 2013–2017, the annual average concentration of PM_{2.5} in Shanxi exceeded about 50% than the second-level limits (35 µg/m³) of the national ambient air quality standard in China—GB 3095–2012 (MEE, 2012). Therefore, we chose a 50% reduction ratio for each of the targeted source category so as to analyze pollutant migration potentials in Shanxi.

The sensitivity from one source category was determined by calculating the difference between the base case and the mitigation case when the emission of this category was set to reduce by 50% using the following equations:

$$C_{i,r} = C_{Base} - C_{i-x} \quad (1)$$

$$P_{i,r} = C_{i,r}/C_{Base} \quad (2)$$

where $C_{i,r}$ and $P_{i,r}$ denote the mitigation potential from category i in terms of concentration and percentage, respectively. C_{Base} and C_{i-x} are the predicted concentrations of the base case and the mitigation scenario case of the emissions reduced by x percent in category i . A similar methodology has been applied in previous studies, particularly for the policy-making (Chen et al., 2019; Cheng et al., 2018; Wang et al., 2012).

2.3. Model evaluation

To evaluate the meteorological results simulated by WRF, we collected the hourly observed meteorological data in Taiyuan Wusu International Airport station (37.73°N, 112.56°E) from the Computational and Information Systems Laboratory at the National Center for Atmospheric Research in Boulder (NCAR, <https://rda.ucar.edu/>) and calculated the mean bias (MB), Pearson correlation coefficient (R) and root mean square error (RMSE), which were defined by previous research (Zhang et al., 2006). Moreover, the detail information of monitoring station was shown in Fig. 1. Monthly evaluation results over the two domains in terms of the simulated temperature, relative humidity, wind speed for Taiyuan (37.73°N, 112.56°E) in 2012 and 2015 are summarized in Table 1. The results show that the near-surface temperature is under-predicted in both domains of 2015, whereas slightly overvalued in 2012. Predictions over Domain 2 at 9 km resolution in terms of MBs agree better with the observations than those at 27 km, with MBs of -1.26°C and -0.53°C for January and July in 2015, comparing to MBs of -1.27°C and -0.63°C , respectively, at 27 km. Relative humidity at 2 m agrees well with the observations with MBs ranging from -1.1% to -5.5% and R ranging from 0.69 to 0.82 for both domains. It is slightly over-predicted in July 2015. Wind speed at 10 m is well reproduced in both domains, with MBs ranging from -0.02 m s^{-1} to 0.74 m s^{-1} , respectively. Meteorological predictions of a fine grid resolution show a better performance.

The comparative results of the daily-average temperature, relative humidity and wind speed at Domains 2 are illustrated in Fig. 2. The predictions indicate that the simulation at Domains 2 basically has

reproduced the meteorological conditions, and the temperature simulation especially featured with a high accuracy. Overall, the results are generally well consistent with previous simulation results (Cheng et al., 2018; Han et al., 2014).

To evaluate pollutant concentration results simulated by CAMx model, we collected the hourly ground-level observed major pollutant concentration data (SO₂, NO₂, PM_{2.5}, and PM₁₀) of 2015 from the China National Environmental Monitoring Centre. Before 2013, daily Air Pollution Index (API) for major urban areas is the only publicly available air quality data in mainland China (Zhang et al., 2012b). Thus for 2012, the PM₁₀ concentrations which were estimated based on daily average API published by MEE were used to evaluate model performance (Streets et al., 2007; Wang et al., 2010; Zhang et al., 2012b; Liu et al., 2020). The corresponding performance statistics are shown in Table S2, including the MFBs, MFEs, and RMSEs, which are recommended as the key statistical performance measures by US EPA (2007). In this study, the MFBs within $\pm 60\%$ and MFEs within 75% are considered to be a satisfactory performance (Wang et al., 2014). Table S2 summarizes the MFBs, MFEs, and RMSEs for the daily pollutant concentrations in the three representative cities of Datong, Taiyuan, and Yuncheng which located from north to south of Shanxi province. The MFBs and MFEs are within the recommended benchmarks in the majority of three cities. The MFBs and MFEs for the daily average PM_{2.5} concentrations are -1.7% to -70.9% and $39.7\%-71.4\%$, while -8.1% to -109.1% and $45.7\%-109.1\%$ for PM₁₀. Regarding the daily average SO₂ and NO₂ concentration, the MFBs and MFEs range from 10.7% to -85.2% , -1.7% to -140.5% and from 38.3% to 90.7% , $38.3\%-140.5\%$, respectively. As shown in Fig. 3 and Fig. S4, the corresponding performance in rural areas is much better than that in the urban centers, mainly because the regional chemical transport models usually underestimate concentrations of primary air pollutants in the urban centers (Zhao et al., 2018), which may be partially influenced by the complex ground-level land-use and roughness conditions. For further evaluate the accuracy of the simulation results in 2012, we compare modeled consequence with other observed data in Taiyuan (shown in Table S3), which shows better consistency. In addition, the satellite-based pollution data such as the Aerosol Optical Depth (AOD) and column mass concentrations of SO₂ and NO₂ (shown in Fig. S2) are used to evaluate the simulation performance. As depicted in Fig. 5 and Fig. S2, the monthly average distribution of the simulated pollutant concentration are well consistent with the satellite-based observations, in particular for SO₂ and NO₂. Furthermore, the sampling data of sulfate, nitrate, ammonium, OC and EC in Taiyuan (TY) and Yuncheng (YC) were applied to verify the accuracy of modeled major chemical components of PM_{2.5}. As presented in Fig. S3, the modeled monthly regional-average chemical composition of PM_{2.5} showed slightly higher concentrations than the observations. This may due to the absence of certain non-homogeneous chemical reactions in the CAMx model and errors in the emission inventory and meteorological simulation (Xu et al., 2020). Moreover, we compare the time series of pollutants from observations and CAMx simulation results for Shanxi in

Table 1
Overall statistics of daily meteorological predictions over Domain1 and Domain2 in Taiyuan (37.73°N, 112.56°E).

Item	2012				2015				
	Jan.		Jul.		Jan.		Jul.		
	D01 (27 km)	D02 (9 km)							
T2 (k)	MB	0.45	0.57	0.06	0.10	-1.27	-1.26	-0.63	-0.53
	RMSE	1.81	1.83	1.39	1.38	1.96	1.96	1.41	1.36
	R	0.78	0.77	0.76	0.76	0.80	0.80	0.86	0.86
WS10 (m s ⁻¹)	MB	0.44	0.75	-0.22	-0.02	0.41	0.74	-0.66	-0.39
	RMSE	0.82	1.02	1.01	0.97	0.88	1.08	1.05	0.92
	R	0.80	0.81	0.43	0.39	0.59	0.59	0.36	0.31
RH (%)	MB	-1.07	-2.20	-5.51	-5.24	-3.94	-4.16	0.80	0.57
	RMSE	7.98	8.31	12.18	12.02	8.38	8.39	7.76	7.98
	R	0.74	0.73	0.69	0.70	0.81	0.82	0.80	0.78

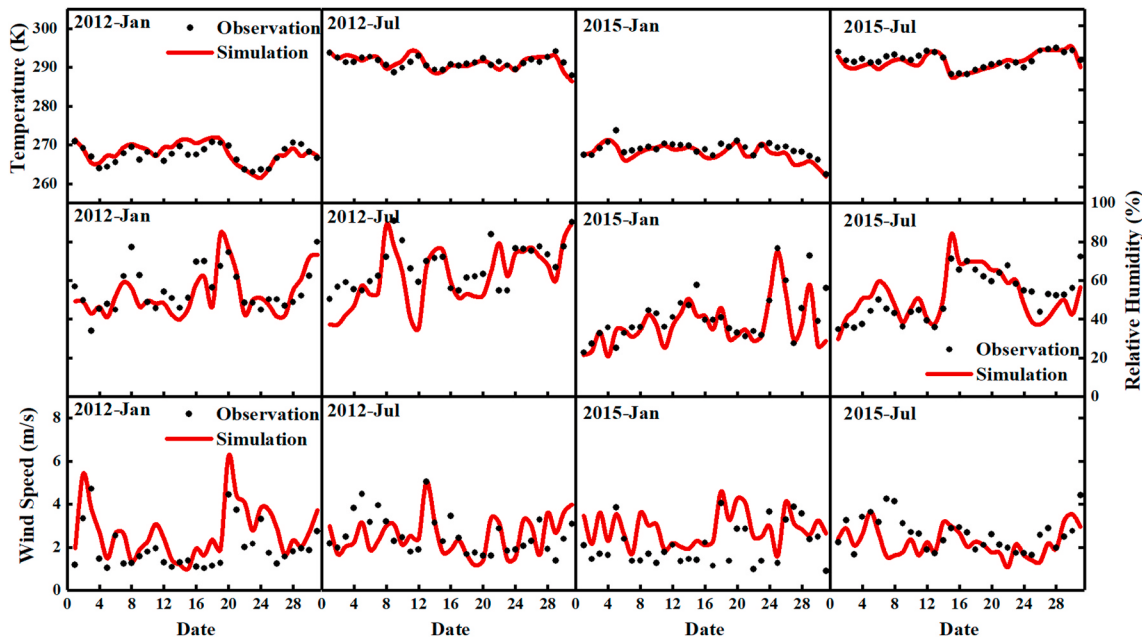


Fig. 2. Time series of observed and modeled daily-average meteorology at Domains 2 in Taiyuan (37.73°N, 112.56°E).

2012 (see SI Figs. S5) and 2015 (Fig. 3 and Fig. S4). The time series and evaluation results indicate that the model under-predicted somewhat the mass concentrations of pollutants, especially for NO₂ and aerosol in July, which may be partly explained by the biases in the meteorological predictions, the lack of fugitive dust and biogenic emissions, the limitation of the special terrain, and the deficiency of model mechanism, respectively. The simulation results of PM_{2.5} are better than those of PM₁₀ and July better than January, because Shanxi Province is susceptible to the dust weather in Inner Mongolia, especially in January. In summary, the above statistics indicate an overall satisfactory performance of predictions. Consequently, the model performance is acceptable to quantify and explore pollution variation and its mitigation potentials in Shanxi.

3. Results and discussion

3.1. Changes of primary air pollutants emissions from 2012 to 2015

In order to meet the targets of APPCAP, the Chinese central government and local government of Shanxi Province released a series of control policies and measures, which had brought a significant improvement in air quality (Cheng et al., 2018). Based on the multi-resolution unit-based emission inventory (Liu et al., 2018a), Shanxi's atmospheric emissions were updated by year and source sector, as shown in Fig. 4, Fig. S7, and Table S4. The primary air pollutant emissions in Shanxi in 2012 were estimated as follows: 563 kt of PM_{2.5}, 1024 kt of PM₁₀, 1920 kt of SO₂, and 1327 kt of NO_x. For PM_{2.5}, PM₁₀, and SO₂, other industries sources (which consist of nonferrous metal smelting plants, waste treatment sources, VOCs product-related sources, other stationary combustion sources, and industrial processes sources), constituted the dominant contributors of the associated total pollutants emissions. Residential use was also major sources of PM_{2.5} and PM₁₀ emissions, accounting for 23.1% and 20.9%, respectively. Followed by other industries sources, power plants represent the second largest category of SO₂ emissions due to huge volume of coal use by power plants. For NO_x, among the major sectors, power plant sector was the dominant contributor with an average contribution of 45.8%, followed by other industries sources (35.7%) and transportation sources (10.5%). As one of the major coal-production bases and intensive energy-consuming provinces in mainland China, the coal consumption

in Shanxi Province accounted for 7.9% and 8.7% of China (China Energy Statistical Yearbook, 2013, 2016), whereas the number of civil vehicles only accounted for 3.0% and 2.9% in 2012 and 2015 (Yearbook of China Transportation and Communications, 2013, 2016), respectively. Thus, the contribution of transportation sources to pollutants, particularly NO_x was not significant compared with Tianjin (~20%) and Beijing (~30%) (Qi et al., 2017), whereas was similar to Lanzhou (~11%) (Zhang et al., 2017b) and Dalian (~14%) (Yuan et al., 2018). Furthermore, the discrepancy of adopted emission factors and available activity level for transportation sources may also lead to underestimation of emissions (Liu et al., 2018a).

Compared with 2012, PM_{2.5}, PM₁₀, SO₂, and NO_x emissions in 2015 were estimated to decrease by about 4.1%, 8.6%, 14.7%, and 4.0%, respectively, under similar total energy consumption and regional GDP levels shown in Table S5. It suggests that the effectiveness of upgrading of industry structure and end-pipe control strategies of pollutant emissions in Shanxi province, meanwhile a great challenge for the balance between keeping economic growth and improving air quality. It was noted that SO₂ emissions decreased sharply than any other primary pollutants, mainly due to the dominant source sectors (i.e., power plants and industry) both significantly reduced their emissions (Zheng et al., 2018).

During 2012–2015, the other industries sector made the greatest contributors to PM_{2.5} and PM₁₀ emission reductions, which decreased PM_{2.5} and PM₁₀ emissions by 35 kt and 47 kt. Reductions in SO₂ emissions mainly came from other industries sector and residential use, with the reduction of 145 kt and 118 kt, respectively. For NO_x emissions reductions, power plants and transportation were the most prominent contributions, with reductions of 39 kt and 24 kt.

Furthermore, the structure of the emission proportions also changed. For PM_{2.5}, other industries sources and residential use remained the greatest emitters in 2015 but represented a higher proportion to residential use and lower to other industries in 2015 than in 2012. With the contributions of SO₂ emission reductions in the residential sector, the proportions of power plants and other industries sources showed a slightly increase. For NO_x, the contribution of power plants decreased from 45.8% to 44.6% in 2015 with the wide application of SCR in coal-fired power plants during the 12th five-year plan (2011–2015).

In summary, the variations in emissions by sector and year were mainly attributable to effective air pollution control policies and

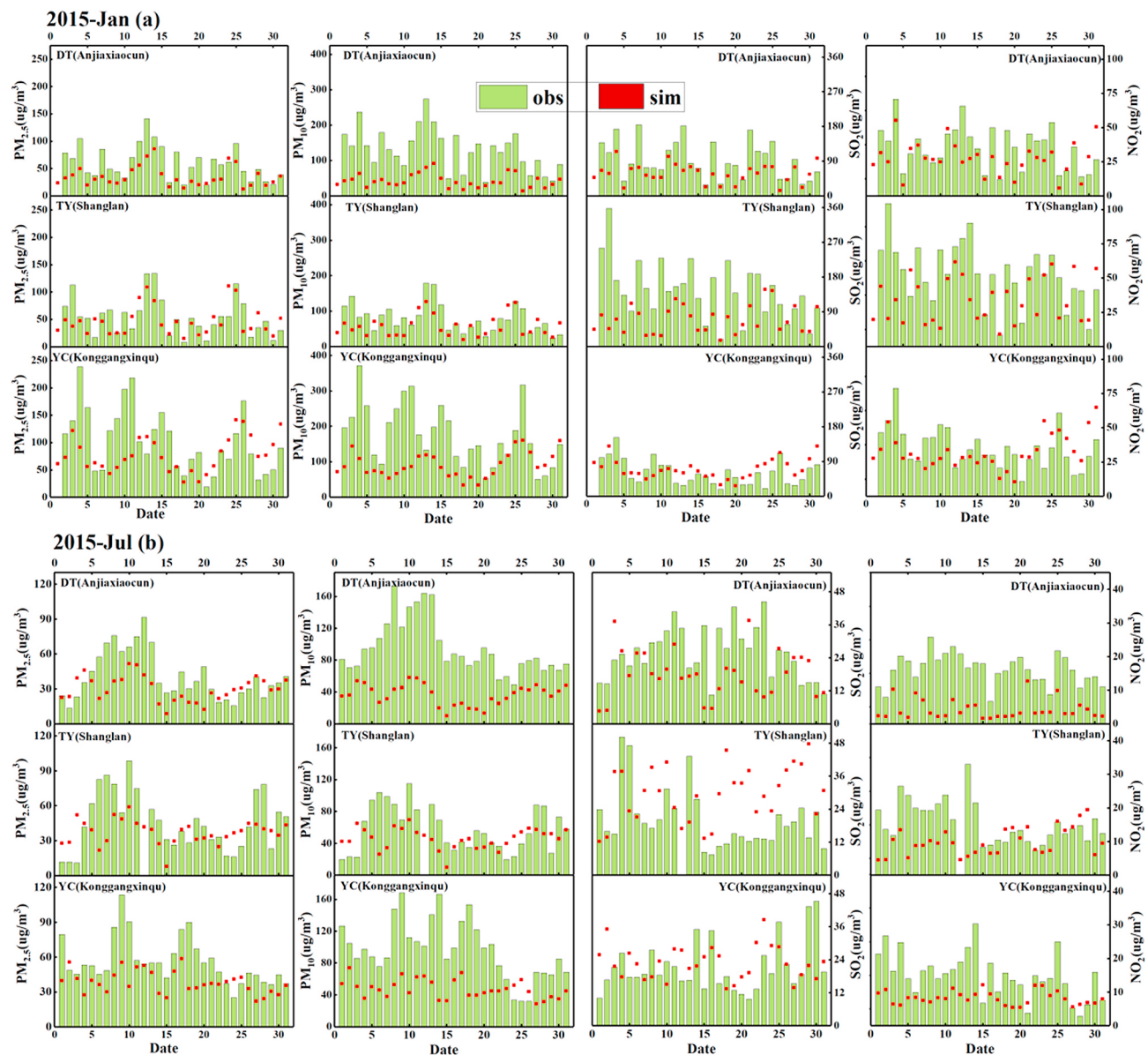


Fig. 3. Observed (green bars) and modeled (red circles) daily mass concentrations ($\mu\text{g}/\text{m}^3$) of $\text{PM}_{2.5}$, PM_{10} , SO_2 and NO_2 in January (a) and July (b) 2015 in rural site at Domain 2. (For interpretation of the references to colour in this figure legend, the reader is referred to the Web version of this article.)

measures, such as phase out outdated industrial capacity, upgrades on industrial boilers, and retire old vehicles. During 2012–2015, more than 1800 small coal boilers were eliminated in Shanxi. In addition, outdated or inefficient technologies and capacity in various industry sectors were phased out during this period. For example, 500 MW coal-fired power generation capacity, 5040 thousand tons of iron and steel production capacity, 4100 thousand tons of cement production capacity, and 12000 thousand tons of coke production capacity were eliminated due to outdated technologies or overcapacity. By the end of 2015, 24 GW, 18 GW, and 24 GW coal-fired power units had upgraded its desulfurization, denitrification, and dust removal facilities, respectively. Apart from the air pollution control policies and measures in industries sectors, the “China IV” emission standard was applied to light gasoline and diesel vehicles in 2015, and about 77 thousand old and “yellow-label” vehicles were eliminated from 2012 to 2015 (The People’s Government of Shanxi Province, 2015). It is worth mentioning that Shanxi province has added about 1366 thousand vehicles from 2012 to 2015 (Yearbook of China Transportation and Communications, 2013, 2016), the positive effect on eliminated “yellow-label” vehicles was largely offset by the rapid

increase of new registered vehicles and the total retention of the vehicles. Therefore, the difference between the transportation emission in 2012 and 2015 was quite limited.

3.2. Changes in spatial and temporal characteristics of pollutants

For a lucid discussion, the average modeled concentrations of primary air pollutants over domain 2 in January and July for the years 2012 and 2015 are depicted in Fig. 5. Consistent with anthropogenic emissions (shown in Fig. S7), very high concentrations of pollutants can be observed in several cities, especially over the urban areas of Taiyuan, Linfen, Jincheng, Changzhi, Luliang, Yangquan, and Jinzhong, which are densely deployed with high energy consumption manufacturing enterprises. Furthermore, as presented in Fig. 1, the topography of those cities is in basin and valleys, which is unfavorable for pollutant dispersion while facilitating pollution accumulation under stagnant meteorological conditions.

There are quite a few differences between January and July. In January, the simulated concentrations of PM_{10} , SO_2 , and NO_2 in those

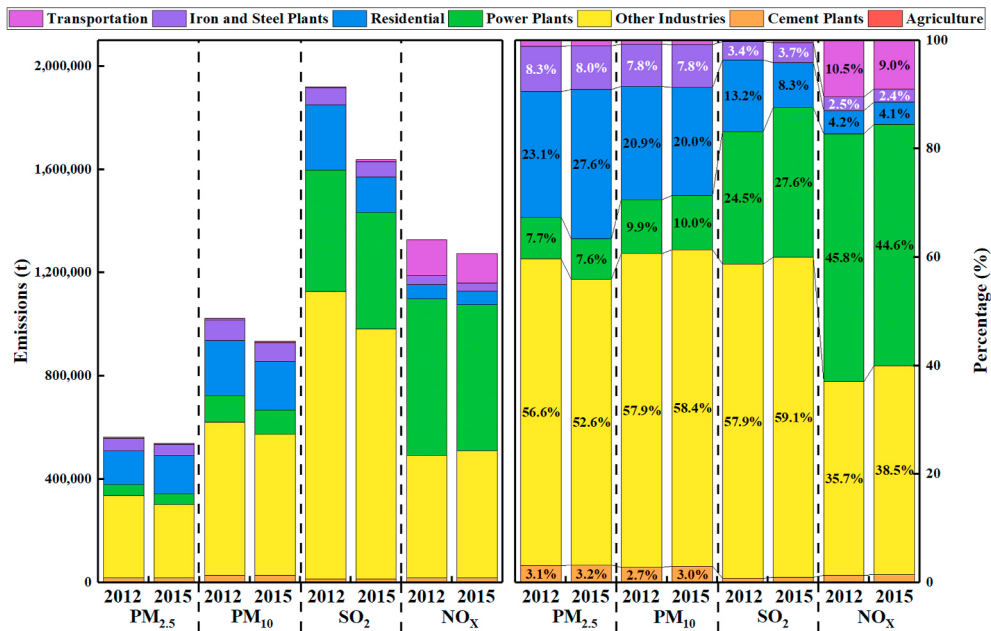


Fig. 4. Changes in anthropogenic emissions of SO₂, NO_x, PM₁₀ and PM_{2.5} in Shanxi for the years 2012 and 2015.

areas are about 100 $\mu\text{g m}^{-3}$, 90 $\mu\text{g m}^{-3}$, and 30 $\mu\text{g m}^{-3}$, respectively. And particularly, predicted daily PM_{2.5} concentrations in those areas are close to or higher than 90 $\mu\text{g m}^{-3}$, which are much higher than the CNAQS daily average PM_{2.5} standard of 75 $\mu\text{g m}^{-3}$. By comparison, the heavily polluted scope in those areas shrinks remarkably accompanying with the decrease of concentration values in July. The predicted concentrations of PM_{2.5}, PM₁₀, SO₂, and NO₂ in heavily polluted areas are close to or higher than 45 $\mu\text{g m}^{-3}$, 50 $\mu\text{g m}^{-3}$, 50 $\mu\text{g m}^{-3}$, and 30 $\mu\text{g m}^{-3}$, respectively. Noticeably, the overall spatial distribution patterns of simulated pollutants concentrations are basically consistent with the spatial distribution of anthropogenic primary air pollutants emissions in Shanxi (Liu et al., 2018a), which described high concentrations occurring in the municipalities and capital cities and suggesting the predominant influence of local emissions on air quality in Shanxi province. Moreover, high concentrations of pollutants can be also found on the east and southeast region out of the Shanxi domain, which covered several top 20 heavily polluted cities (like Shijiazhang, Xingtai, Handan, Anyang, Jiaozuo and Xinxiang) located in the eastern foot of Taihang Mountains, as showed in Fig. 5, suggesting non-negligible transportation of pollutants from areas outside this domain during the simulation period (Wang et al., 2017b).

Compared with 2012, both the pollution areas and spatial distribution pattern do not display noteworthy changes in 2015. However, as shown in Fig. 5, the monthly average concentrations of primary air pollutants have presented an obvious declining variation trend from 2012 to 2015.

In January of winter which featured with elevated space heating demand, the simulated monthly average concentrations of PM_{2.5}, PM₁₀, SO₂ and NO₂ in 2012 are 58.38 $\mu\text{g m}^{-3}$, 68.38 $\mu\text{g m}^{-3}$, 67.73 $\mu\text{g m}^{-3}$ and 27.52 $\mu\text{g m}^{-3}$, while they are decreased to 43.95 $\mu\text{g m}^{-3}$, 51.89 $\mu\text{g m}^{-3}$, 52.18 $\mu\text{g m}^{-3}$, and 22.58 $\mu\text{g m}^{-3}$ in 2015, reduced by 24.7%, 24.1%, 23.0% and 18.0%, respectively.

By contrast, in July of summer, the predicted monthly concentrations of PM_{2.5}, PM₁₀, SO₂, and NO₂ in 2012 are about 32.91 $\mu\text{g m}^{-3}$, 40.68 $\mu\text{g m}^{-3}$, 25.60 $\mu\text{g m}^{-3}$, and 8.06 $\mu\text{g m}^{-3}$, while they are reduced to about 34.05 $\mu\text{g m}^{-3}$, 41.90 $\mu\text{g m}^{-3}$, 24.74 $\mu\text{g m}^{-3}$, and 6.86 $\mu\text{g m}^{-3}$ in July of 2015, respectively. It is worth mentioning that compared with 2012, the simulated concentrations of SO₂ and NO₂ are only reduced by about 3.4% and 14.8% in July of 2015, which is much smaller than the variation ratios in January, and especially, the simulated concentration of

PM_{2.5} and PM₁₀ are even increased by about 3.4% and 2.9%, respectively. The increase of simulated concentrations for particulate matters mainly appear in the areas of Jincheng, Linfen, Jinzhong, Yuncheng, and Changzhi, which are closely related to the increase of primary emissions of PM_{2.5} and PM₁₀ mainly from residential, as presented in Table S4. In addition, the influence of meteorological conditions cannot be ignored, which is discussed in detail below.

3.3. Variation of major aerosol components in PM_{2.5} and its associations with meteorological conditions

Fig. 6 presents the modeled time series of regional-average temperature, relative humidity, surface wind speed, the mass concentrations of PM_{2.5}, as well as the average contribution ratios of sulfate, nitrate, ammonium, EC, OC, and others components to Shanxi province in January and July for the years 2012 and 2015, respectively. The conditions of meteorological, such as temperature, relative humidity, and surface wind speed are the important factors influencing changes of simulated mass concentrations of PM_{2.5} (Wang et al., 2017b). As shown in Fig. 6b and f, compared with 2012, the unfavorable meteorological conditions with lower wind velocity and higher temperature and humidity appeared in 2015, which maybe represent another reason for interpreting the increase of simulated PM_{2.5} concentrations in July.

As illustrated in Fig. 6, higher mass concentration of PM_{2.5} corresponds to a higher contribution ratio of the secondary inorganic aerosols (SIA) including sulfate, nitrate, and ammonium. Moreover, variation trends of PM_{2.5} concentration match with the contribution ratio of SIA very well, especially for January. This feature confirms that nitrate, sulfate, and ammonium have constituted major aerosol components that influenced the heavy haze formation and evolution processes in Shanxi. The predominant component of PM_{2.5} is sulfate in July, mainly because the photochemical reactions and 'gas-particle' conversions are enhanced under the higher temperatures and increased humidity in summer season (Zhang et al., 2018). However, rather than sulfate, the dominant component of PM_{2.5} in January is transformed into nitrate, even though the concentrations of gaseous NO₂ are much lower than SO₂ as shown in Fig. S6. This seasonal variation phenomenon is similar to the previous studies about Beijing, Yangquan, and Taiyuan as shown in Table S6. The most likely reason for this feature is that high-frequency stagnant weather and low temperature in winter restrains the diffusion of air

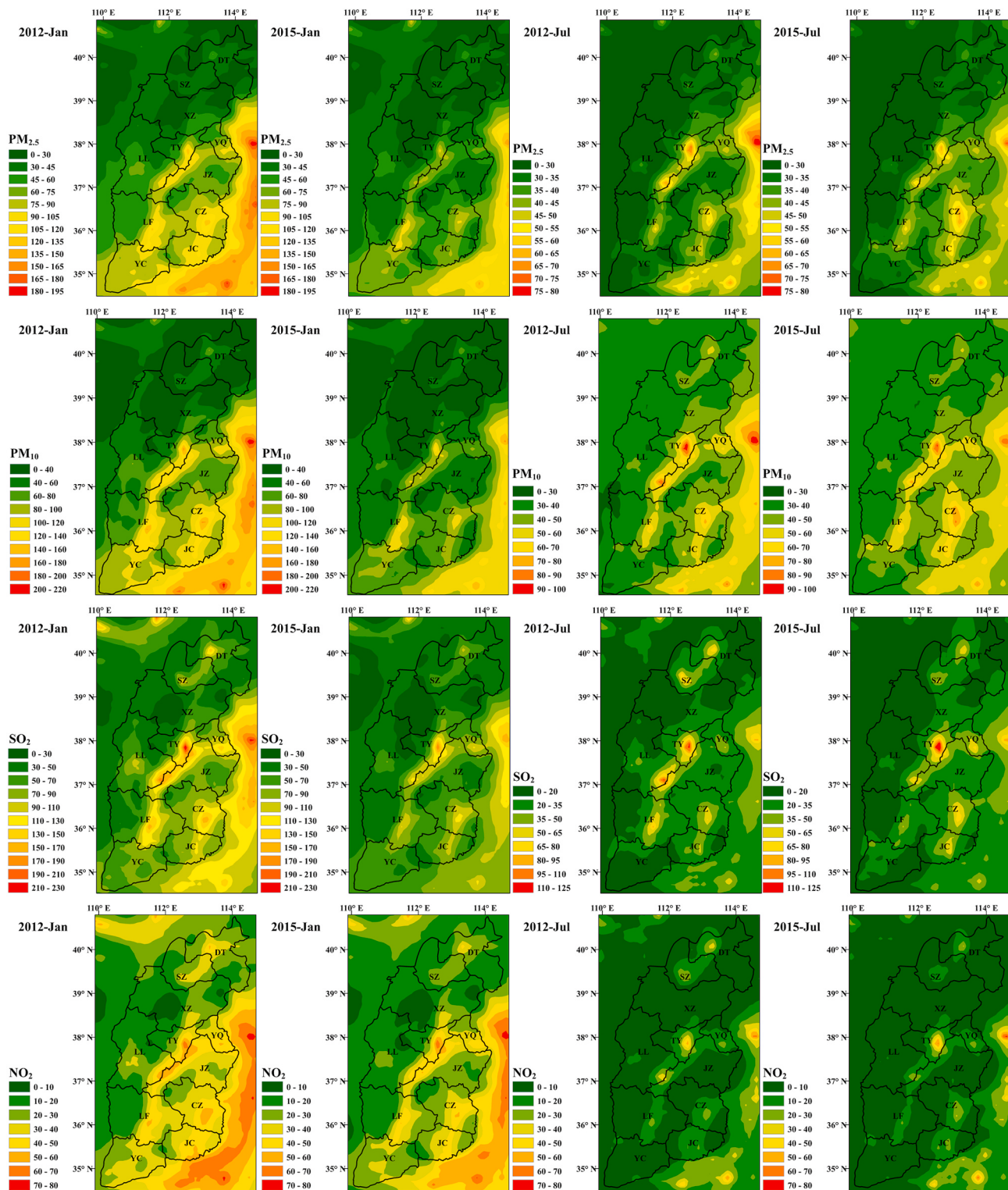


Fig. 5. Spatial distributions of monthly-average simulated mass concentration of $\text{PM}_{2.5}$ ($\mu\text{g}/\text{m}^3$), PM_{10} ($\mu\text{g}/\text{m}^3$), SO_2 ($\mu\text{g}/\text{m}^3$) and NO_2 ($\mu\text{g}/\text{m}^3$) in January and July for the years 2012 and 2015.

pollutants and promotes the gas-to-particle conversion of NO_2 to nitrate (Zhang et al., 2017a; Jia et al., 2018), which deserves further investigation for better understandings.

As shown in Table 2, the SIA significantly contributes to the $\text{PM}_{2.5}$ pollution, which is over 49%. This value is comparable with the previously simulated results (Han et al., 2014; Zhang et al., 2018). In addition, the high contribution of ammonium appears in winter, mainly

driven by the markedly increased emissions of SO_2 in winter, and it combines with NH_3 to produce a large amount of $(\text{NH}_4)_2\text{SO}_4$ in the atmosphere (Zhang et al., 2017a). The contribution of carbonaceous aerosol, including EC and OC, is high in January and relatively low in July. These seasonal patterns are similar as those of Beijing and Tangshan found in previous studies (Han et al., 2014; Zhang et al., 2018).

In addition to the unfavorable diffusion conditions, the strong

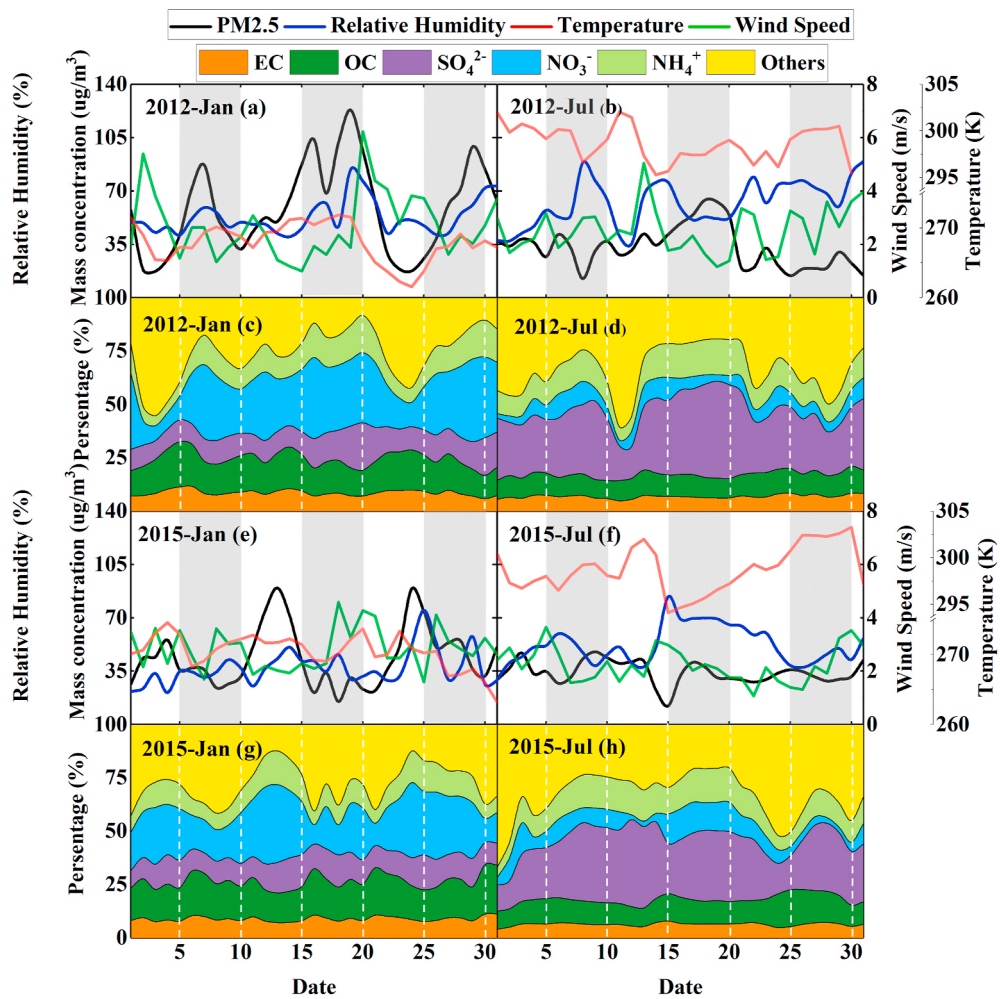


Fig. 6. The simulated time series of the regional-average relative humidity (%), temperature (K), surface wind speed (m/s) and $\text{PM}_{2.5}$ mass concentrations ($\mu\text{g}/\text{m}^3$) in January and July for the years 2012 and 2015 in Shanxi (a, b, e, f), and extinction contribution ratios (c, d, g, h) of sulfate, nitrate, ammonium, EC, OC, and others (dust and unspecified anthropogenic discharges).

Table 2

Mass concentrations ($\mu\text{g}/\text{m}^3$) and contribution ratios (%) of SIA, OC, EC, and Others (dust and unspecified anthropogenic discharges) to $\text{PM}_{2.5}$ in Shanxi.

Variables	2012-Jan	2012-Jul	2015-Jan	2015-Jul	Δ Jan(2015–2012)	Δ Jul(2015–2012)
	Mass concentration ($\mu\text{g}/\text{m}^3$) (contribution ratio (%))					
SIA	32.47 (55.62)	16.89 (51.32)	21.69 (49.35)	16.69 (49.02)	-10.78 (-6.27)	-0.20 (-2.30)
SO_4^{2-}	7.70 (13.19)	10.50 (31.91)	5.46 (12.42)	9.66 (28.37)	-2.24 (-0.77)	-0.84 (-3.54)
NO_3^-	17.11 (29.31)	2.08 (6.32)	11.11 (25.28)	2.76 (8.11)	-6.00 (-4.03)	+0.68 (+1.79)
NH_4^+	7.66 (13.12)	4.31 (13.10)	5.12 (11.65)	4.27 (12.54)	-2.54 (-1.47)	-0.04 (-0.56)
OC	8.87 (15.19)	3.33 (10.12)	7.58 (17.25)	3.90 (11.45)	+8.38 (+2.06)	+0.57 (+1.33)
EC	4.83 (8.27)	2.19 (6.65)	3.83 (8.71)	2.12 (6.23)	-1.00 (+0.44)	-0.42 (-0.42)
Others	12.21 (20.91)	10.50 (31.91)	10.85 (24.69)	11.34 (33.30)	-1.36 (+3.78)	+0.84 (+1.39)

emission intensity of coal and biomass burning for space heating are the main reasons for the carbonaceous aerosol values remaining high levels during the winter (Zhang et al., 2014). Moreover, the contribution of other sources, including dust and unspecified anthropogenic discharges was about 30%, which cannot be neglected and deserve further investigations.

As shown in Table 2, from 2012 to 2015, mass concentrations and contribution ratios of most components in $\text{PM}_{2.5}$ are decreased, which are well consistent with the variation characteristics of emissions inventory as presented in Section 3.1. Moreover, Table 2 illustrates the slight growth of nitrate in July during 2012 to 2015. Such a rising trend is possibly correlated with the growing number of civil motor vehicles in

Shanxi with a growth rate of 29.8% during 2012 to 2015, as well as the unfavorable meteorological conditions as shown in Fig. 2.

3.4. Contribution transformation of different sectors to air pollution

To develop the practical and effective emission control strategy, it is very crucial to both qualitatively and quantitatively identify which emission sectors are more sensitively responsible for pollution formation and reduction. The average contributions by source sector to the pollutant concentrations in typical prefecture-level cities of Shanxi province in January and July for the years 2012 and 2015 are presented in Fig. 7 and Fig. S8. As shown in Fig. 7a, except for pollution caused by

local emission, the average contributions from surrounding regions outside of Shanxi cannot be ignored, with the concentration contributions of 51.5% to $\text{PM}_{2.5}$ and 48.9% to PM_{10} , particularly. This phenomenon showed comparable quantity with previous study (Li et al., 2019), with the regional contributions of 63.72% and 51.87% to $\text{PM}_{2.5}$ across Shanxi in January and July, respectively. As discussed above, the main reason is illustrated in Fig. 5, showing that the concentration of pollutants in Hebei and other surrounding areas is higher than that in the neighboring cities of Shanxi. Thus, it suggests that trans-provinces pollution transportation may occur from Hebei to Shanxi under eastern wind flow in July (shown in Fig. S9), although the high-altitude Taihang Mountains which stretched from north to south have played a good role as a barrier between the two provinces. In addition, transportation from the northwest of Henan and the southwest of Shaanxi provinces calls for further study in the future.

There are quite a few differences between January and July. In January, the most important sector to $\text{PM}_{2.5}$ is residential (19.1%), followed by other industries (17.3%). The contributions of power plants, transportation, cement plants, iron and steel plants, and agriculture sources are all less than 10%. By contrast, all seven sectors show comparable contributions in July, and the share of other industries sector is most prominent (23.9%). For PM_{10} , other industries and residential sources are responsible of the top two major sectors in January across Shanxi, accounting for 21.8% and 19.6%, respectively. When the contribution is declined from January to July for residential sources due to no demand for winter-season space heating, other industries sector which is largely operated in year-round became the major sources of PM_{10} in July, sharing with 25.8%.

The major sources for SO_2 in January are other industries sector, residential sector, and power plants, with a combined contribution of 69.3%. Whereas, other industries sectors and power plants together contribute about 74.7% of SO_2 in July, mainly due to the substantial decrease of emissions from residential use for heating. In addition, the major sources for NO_2 include other industries sector, power plants, and

transportation sector, with collective contributions from 81.9% in January to 92.2% in July. Seasonal diversities of the contributions from different source categories are caused by the seasonal variations of both emission intensities and meteorological conditions. The residential source including cooking and heating, and the latter mainly happens in winter (Streets et al., 2003). As a result, residential sources emit more than 3 times in winter of in summer for $\text{PM}_{2.5}$, PM_{10} , SO_2 and NO_2 across Shanxi. In addition, due to the high emissions, the contributions of other industries sector are larger than residential sector in pollutants except for $\text{PM}_{2.5}$, although the pollutants from residential sector are mainly emitted by low chimney near the ground, and thus more easily pose higher harm influence than the industry sources normally discharge with elevated stack (Zhao et al., 2017b). In contrast, agricultural emissions are usually high in summer when the temperature is high and fertilizer is widely used (Fu et al., 2015). Generally, primary gaseous and particulate emissions from elevated-stacks such as power plants, cement plants and iron and steel plants may contribute the high background concentrations as well as supply enough precursors for secondary aerosols formation in a large-scale region.

The relative contribution for each city varies from each other in Shanxi province. As shown in Fig. 7b-d and Fig. S8, the regional contributions from Datong, Xinzhou and Yuncheng are higher than other prefecture-level cities, because they are located in the north or south transmission channels in Shanxi basin, respectively (see Fig. 1). For $\text{PM}_{2.5}$, the dominant source in January is residential sector for Datong, Linfen, Shuozhou, Taiyuan, Xinzhou, Yangquan, Yuncheng, while other industries sector is predominant for Jincheng, Lvliang, Jinzhong, and Changzhi, respectively. However, for PM_{10} , residential sector represents the dominant contributor for Datong, Shuozhou, Xinzhou, and Yuncheng, while other industries sector is pronounced for other prefecture-level cities.

For SO_2 , the most important sector is other industries sources for all prefecture-level cities, followed by power plants for Datong, Jincheng, Shuozhou, Xinzhou, Jinzhong, and Changzhi, while it is followed by

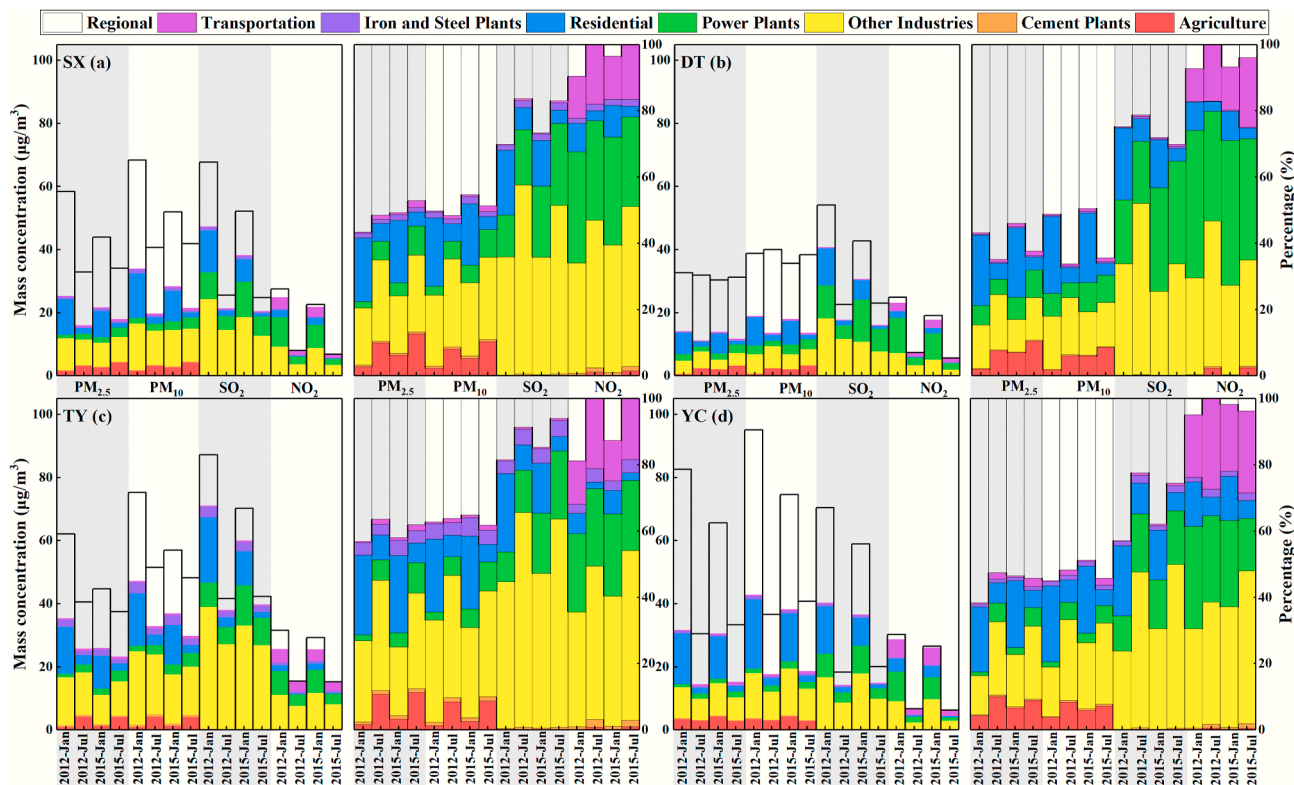


Fig. 7. Source contributions by different sectors to pollutant concentrations in (a) SX, (b) DT, (c) TY, and (d) YC in January and July for the years 2012 and 2015.

residential sources for Lvliang, Linfen, Taiyuan, Yangquan and Yuncheng. In addition, for NO_2 , the dominant source is power plants for Datong, Shuzhou and Xinzhou, while it changes into other industries sector for other remaining prefecture-level cities.

As depicted in Fig. 7 and Fig. S8, contributions of different sectors have showed noticeable variations from 2012 to 2015. Along with the improvement of air quality in surrounding areas of Shanxi since the enacting of APPCAP in 2013, the regional contributions have also decreased by 2015. For local sources, the contributions of other industries sector to pollutants, especially for SO_2 has showed a decreasing trend during 2012–2015 in most cities of Shanxi. However, the contributions of power plants to primary air pollutants in 2015 are observed to be slightly higher than that in 2012, mainly due to the obvious decrease of sector contributions from other industries following the implementation of effectiveness pollutants reductions measures, as discussed in Section 3.1.

3.5. Mitigation potential of pollutant emissions in Shanxi

Scenario simulation results on mitigation potentials of average pollutant emissions are shown in Fig. 8 and Table S7.

As illustrated in Fig. 8, the emission control of residential use sector has the greatest potential for $\text{PM}_{2.5}$ pollution mitigation of $3.35 \mu\text{g}/\text{m}^3$ (7.04%) in January, followed by other industries sources sector with a mitigation potential of $2.98 \mu\text{g}/\text{m}^3$ (5.96%), and potentials of power plants and agriculture sector are at similar levels of about $0.50 \mu\text{g}/\text{m}^3$ (~1.30%). In July, however, the sector with greatest potential changes into other industries with $\text{PM}_{2.5}$ pollution mitigation of $2.69 \mu\text{g}/\text{m}^3$ (7.45%), followed by power plants and agriculture sources of about $1.00 \mu\text{g}/\text{m}^3$ (~3.00%), while the potential of residential sources is only $0.56 \mu\text{g}/\text{m}^3$ (1.57%), because the majority of residential sector emission is mainly happened in winter. It is noteworthy that the ranking consequence of emission reduction potential is consistent with the results of sector contribution.

In addition, due to the high sector contribution, potentials for SO_2 pollution mitigation from the emission control of other industries sector, power plants and residential sector are higher than other sources, whose mitigation potentials are about $8.13 \mu\text{g}/\text{m}^3$ (13.86%), $4.64 \mu\text{g}/\text{m}^3$ (9.34%), and $2.81 \mu\text{g}/\text{m}^3$ (5.04%) in January, while become $5.36 \mu\text{g}/\text{m}^3$

(19.87%), $2.68 \mu\text{g}/\text{m}^3$ (10.91%), and $0.41 \mu\text{g}/\text{m}^3$ (1.66%) in July, respectively.

For NO_2 pollution mitigation, the emission control is more effective in sectors of other industries, power plants, residential and transportation, whose reduction values are about $3.36 \mu\text{g}/\text{m}^3$ (13.94%), $2.61 \mu\text{g}/\text{m}^3$ (12.65%), $0.90 \mu\text{g}/\text{m}^3$ (3.84%), and $0.86 \mu\text{g}/\text{m}^3$ (3.66%) in January, while the values become $1.57 \mu\text{g}/\text{m}^3$ (20.38%), $0.89 \mu\text{g}/\text{m}^3$ (13.34%), $0.11 \mu\text{g}/\text{m}^3$ (1.57%), and $0.46 \mu\text{g}/\text{m}^3$ (6.33%) in July, respectively. Compared with other sectors, the mitigation potential for pollutant contamination from cement plants and iron & steel plants is much lower in Shanxi, but it shows a higher potential to reduce NO_2 concentrations in Taiyuan, Linfen, and Changzhi compared with other prefecture-level cities.

As depicted in Fig. 8b, emission control of various sectors is universally more effective for pollutant contamination mitigation in summer than in winter, which agrees well with the previous study for Beijing-Tianjin-Hebei region (Wu et al., 2017). A potential explanation includes that the higher temperature and PBL in July are favorable for vertical and horizontal diffusion (Wu et al., 2017) and more precipitation occasions promote the wet deposition of pollutants in summer, whereas the ambient higher humidity in January promoted aerosol heterogeneous chemistry and stable meteorological conditions increased the residence time of precursors, such as SO_2 , NO_x in winter (Guan et al., 2019; Le et al., 2020). Particularly, emission control in summer is significantly more effective for the several sectors like other industries, power plants, and transportation. Power plants and industry sectors emissions are discharged with elevated stack and the near-ground local air quality is less affected in winter, particularly in nighttime when the mixing layer is usually low (Chang et al., 2019). Agriculture sources sector presents a greater contribution emission reduction in summer since substantial emissions from straw open burning occur during this period. Furthermore, the possible causes for the negative potential of pollution reduction include some other factors, such as the weakness of chemical transformation model (CTM) in the treatment of the heterogeneous $\text{PM}_{2.5}$ formation in the atmosphere (Wang et al., 2014).

It is of great significance to identify the main control sectors in each city for improving regional environmental air quality. As shown in Table S7, priorities should be given to $\text{PM}_{2.5}$ and PM_{10} emission control

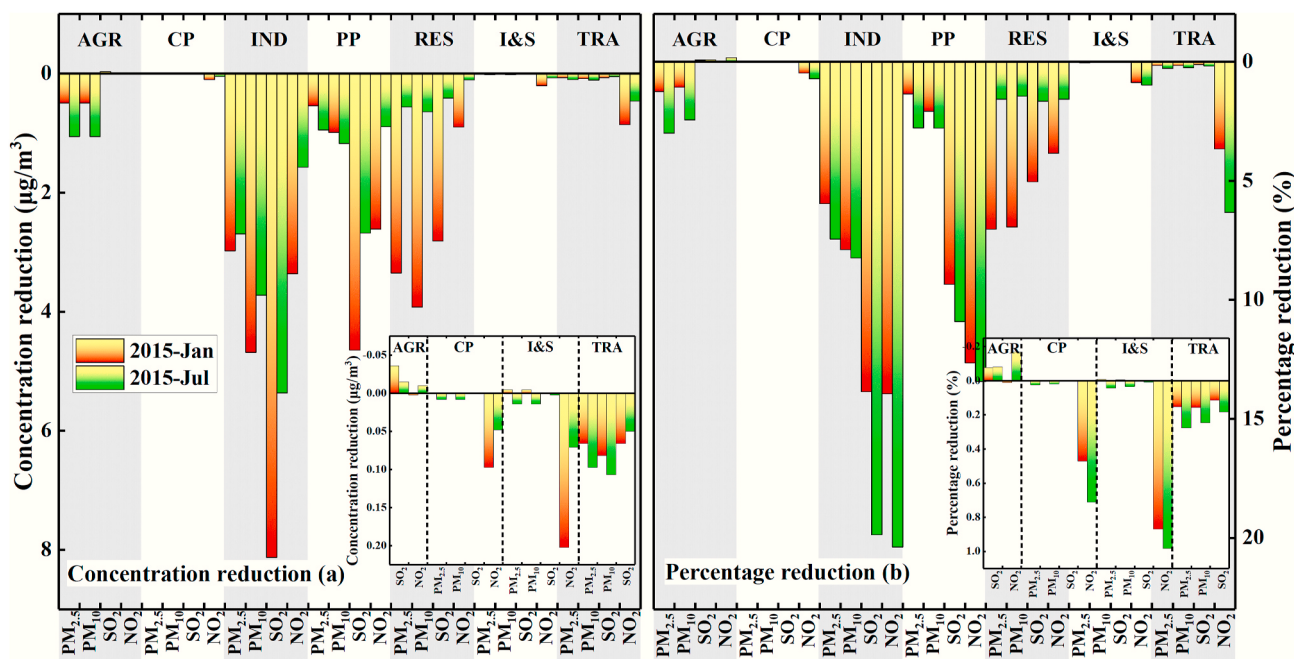


Fig. 8. Changes of regional average pollutants concentration (a) and percentage (b) reduction under 50% emission mitigation from major emission sectors in Shanxi.

for other industries sector and residential sector in January, the former is identified to show the greatest potential to reduce emissions in Jincheng, Lvliang, Linfen, Taiyuan, Yangquan, Jinzhong, and Changzhi, respectively, while the latter possesses the greatest potential in Datong, Shuozhou, Xinzhou, and Yuncheng. In addition, in July, more attention should be devoted to controlling the pollutant emissions from other industries sector, and the sectors of power plants and agriculture at Datong, Shuozhou, Xinzhou, Jinzhong, and Changzhi should be noticed besides. Moreover, in terms of reducing the concentration of SO₂ and NO_x, tighter emission standards should be further applied to power plants and effective emission control measures should be taken in industry (including iron & steel plants, cement plants, and other industries sector) in January and July across all prefecture-level cities, suggesting and confirming the necessities of implementing ultra-low emission retrofitting not only in coal-fired power plants, but also strengthening the emission control for heavy manufacturing industries like iron & steel smelting, coal coking and cement plants. In addition, fugitive dust (soil, industrial and domestic material piles, construction sites and traffic dust) as well as unorganized workshop emissions of PM and gaseous pollutants (VOCs, NH₃, SO₂, NO_x, etc.) should also be highlighted and enforced in order to further improve air quality.

4. Conclusions

In this study, the evolution of spatial-temporal distribution characteristics, source contribution, and mitigation potentials of primary air pollutants in Shanxi were investigated. Based on the multi-resolution unit-based emission inventory, the primary emissions of PM_{2.5}, PM₁₀, SO₂, and NO_x in Shanxi had been reduced by about 4.1%, 8.6%, 14.7%, and 4.0% from 2012 to 2015. Owing to the emissions reduction and favorable meteorological conditions, the simulated monthly average concentrations of PM_{2.5}, PM₁₀, SO₂, and NO₂ are reduced significantly from 2012 to 2015 especially in January. In contrast, no remarkable variations are observed in terms of both the pollution areas and its spatial distribution pattern. From 2012 to 2015, mass concentrations and contribution ratios of most chemical components in PM_{2.5} have been decreased, whereas the SIA (including sulfate, nitrate, and ammonium) still represents the major aerosol component with the proportion of about 49%. In addition, during the haze periods, the increase in PM_{2.5} concentration is highly driven by secondary SIA formation and accumulation originated both from homogeneous and heterogeneous atmospheric chemical reactions.

Other industries sector, residential use, and power plants constitute the major local contributors to primary air pollutants concentrations, and the contribution of transportation sources to NO₂ is also significant, especially in urban areas with densely residents and traffic jam. Furthermore, since the high concentration of pollutants occasionally appears in surrounding areas, the regional contributions to air pollution in Shanxi cannot be ignored. It suggests that enhanced emission control and air quality improvement in surrounding provinces (like Hebei, Henan, and Shaanxi) have also positively contributed the air quality improvement in Shanxi, and further reveals the changes of structure of the sector emission proportion following the implementation of APP-CAP. For further improve regional air quality in Shanxi, suitable and effective seasonal-specific emission reduction measures in each prefecture-level city is much more important, such as priorities should be given to PM_{2.5} and PM₁₀ emission control in January for other industries sector in Jincheng, Lvliang, Linfen, Taiyuan, Yangquan, Jinzhong, and Changzhi; whereas highlights residential sector in Datong, Shuozhou, Xinzhou, and Yuncheng. In addition, in July, more attention should be devoted to reducing the pollutant emissions from other industries sector, and the sectors of power plants and agriculture at Datong, Shuozhou, Xinzhou, Jinzhong, and Changzhi should be highlighted at the same time. For reducing the concentration of SO₂ and NO₂, the effective emission control measures should be taken in combustion sources including power plants and industry sector in January and July

across all prefecture-level cities. Moreover, emission reduction in summer is generally more effective than in winter that merits attention as well.

This study has several limitations. First, limitations in emissions (e.g., the lack of dust emissions and biogenic emissions) may be propagated to the model under predictions of pollutant concentrations. Second, due to the limitation of the SOAP scheme, secondary organic aerosol (SOA) is not well considered in the quantification of sector contributions. Overall, biogenic and fugitive dust emissions should be incorporated into the emission inventory system for better-predicted pollutant concentrations. Finally, it is of great significance for further quantifying various air pollution migration potentials from different sectors based on cost-benefit analysis so as to help promulgate more effective city-specific and sector-specific emission control measures.

CRediT authorship contribution statement

Xiaoxuan Bai: Conceptualization, Methodology, Software, Investigation, Writing - original draft. **Hezhong Tian:** Conceptualization, Data curation, Formal analysis, Writing - review & editing, Supervision. **Xiangyang Liu:** Validation, Visualization, Software. **Bobo Wu:** Validation, Visualization, Software. **Shuhan Liu:** Validation, Formal analysis, Visualization. **Yan Hao:** Data curation, Writing - review & editing. **Lining Luo:** Formal analysis, Visualization. **Wei Liu:** Formal analysis, Visualization. **Shuang Zhao:** Formal analysis, Visualization. **Shumin Lin:** Formal analysis, Visualization. **Jiming Hao:** Formal analysis, Writing - review & editing. **Zhihui Guo:** Writing - review & editing. **Yunqian Lv:** Writing - review & editing.

Declaration of competing interest

The authors declare that they have no known competing financial interests or personal relationships that could have appeared to influence the work reported in this paper.

Acknowledgments

This work was funded by the Trail Special Program of Research on the Cause and Control Technology of Air Pollution under the National Key Research and Development Plan of China (2019YFC0214201, 2018YFC0213202), the National Natural Science Foundation of China (21777008, 51678056), and the National Key Scientific and Technological Project on Formation Mechanism and Control of Heavily Air Pollution (DQGG0209). We would like to acknowledge the editors and anonymous reviewers for their valuable suggestions and comments for improving this paper. The detailed methodologies and source data on developing emission inventory for this research are available in our previous study (<https://www.sciencedirect.com/science/article/pii/S1352231018301511>). Moreover, the hourly observed air pollutants data are accessed via the China National Environmental Monitoring Centre website (<http://www.cnemc.cn/>). The hourly observed meteorology data can be download from the Computational and Information Systems Laboratory at the National Center for Atmospheric Research in Boulder (NCAR) website (<https://rda.ucar.edu/>). The altitude data for the study area are available from the Resource and Environment Data Cloud Platform in China (<http://www.resdc.cn/data.aspx?DATAID=200>). The satellite-based AOD data, SO₂ data, and NO₂ data are accessed from <https://disc.gsfc.nasa.gov/>, <https://giovanni.gsfc.nasa.gov/>, and <http://www.temis.nl/index.php>, respectively. The Weather research and forecasting (WRF v3.7) model is from <https://www.mmm.ucar.edu/wrf-release-information> website. The Comprehensive air quality model with extensions (CAMx 6.4) is from <http://www.camx.com/> website.

Appendix A. Supplementary data

Supplementary data to this article can be found online at <https://doi.org/10.1016/j.atmosenv.2020.117926>.

References

- Anderson, J.O., Thundiyil, J.G., Stolbach, A., 2012. Clearing the air: a review of the effects of particulate matter air pollution on human health. *J. Occup. Med. Toxicol.* 8, 166–175.
- Bo, X., Xue, X.D., Xu, J., Du, X.H., Zhou, B.H., Tang, L., 2019. Aviation's emissions and contribution to the air quality in China. *Atmos. Environ.* 201, 121–131.
- Cai, S.Y., Wang, Y.J., Zhao, B., Wang, S.X., Chang, X., Hao, J.M., 2017. The impact of the "air pollution prevention and control action plan" on PM_{2.5} concentrations in jing-jin-ji region during 2012–2020. *Sci. Total Environ.* 580, 197–209.
- Chang, X., Wang, S.X., Zhao, B., Xing, J., Liu, X.X., Wei, L., Song, Y., Wu, W.J., Cai, S.Y., Zheng, H.T., Ding, D., Zheng, M., 2019. Contributions of inter-city and regional transport to PM_{2.5} concentrations in the Beijing-Tianjin-Hebei region and its implications on regional joint air pollution control. *Sci. Total Environ.* 660, 1191–1200.
- Chen, T.F., Chang, K.H., Lee, C.H., 2019. Simulation and analysis of causes of a haze episode by combining CMAQ-IPR and brute force source sensitivity method. *Atmos. Environ.* 218.
- Cheng, J., Su, J.P., Cui, T., Li, X., Dong, X., Sun, F., Yang, Y.Y., Tong, D., Zheng, Y.X., Li, J.X., Zhang, Q., He, K.B., 2018. Dominant role of emission reduction in PM_{2.5} air quality improvement in Beijing during 2013–2017: a model-based decomposition analysis. *Atmos. Chem. Phys.* 1–31.
- China Energy Statistical Yearbook, 2013. China Statistical Press, Beijing.
- China Energy Statistical Yearbook, 2016. China Statistical Press, Beijing.
- Colella, P., Woodward, P.R., 1984. The piecewise parabolic method (PPM) for gas-dynamical simulations. *J. Comput. Phys.* 54, 174–201.
- ENVIRON, 2016. User's guide for the comprehensive air quality model with extensions (CAMx). Version 6. 30. ENVIRON International Corporation.
- Fu, X., Wang, S.X., Ran, L.M., Pleim, J.E., Coote, E., Bash, J.O., Benson, V., Hao, J.M., 2015. Estimating NH₃ emissions from agricultural fertilizer application in China using the bi-directional CMAQ model coupled to an agro-ecosystem model. *Atmos. Chem. Phys.* 15, 6637–6649.
- Guan, L., Liang, Y.L., Tian, Y.Z., Yang, Z.R., Sun, Y.M., Feng, Y.C., 2019. Quantitatively analyzing effects of meteorology and PM_{2.5} sources on low visual distance. *Sci. Total Environ.* 659, 764–772.
- Han, X., Zhang, M., Gao, J., Wang, S., Chai, F., 2014. Modeling analysis of the seasonal characteristics of haze formation in Beijing. *Atmos. Chem. Phys.* 14, 10231–10248.
- Health Effects Institute, 2019. State of Global Air 2019 Special Report. Health Effects Institute, Boston, MA.
- Jia, J., Han, L.H., Cheng, S.Y., Zhang, H.Y., Lv, Z., 2018. Pollution characteristic of PM_{2.5} and secondary inorganic ions in Beijing-Tianjin-Hebei region. *China Environ. Sci.* 801–811.
- Kain, J.S., 2004. The Kain-Fritsch convective parameterization: an update. *J. Appl. Meteorol.* 43, 170–181.
- Le, T.H., Wang, Y., Liu, L., Yang, J.N., Yung, Y.L., Li, G.H., Seinfeld, J.H., 2020. Unexpected air pollution with marked emission reductions during the COVID-19 outbreak in China. *Science* 369, 702–706.
- Li, H.Y., Gao, X.Y., Li, H.Y., Yan, Y.L., Guo, L.L., He, Q.S., 2018. Spatial-temporal distribution and variation characteristics of PM_{2.5} in Shanxi. *Environ. Chem.* 37, 913–923.
- Li, R., Mei, X., Wei, L.F., Han, X., Zhang, M.G., Jing, Y.Y., 2019. Study on the contribution of transport to PM_{2.5} in typical regions of China using the regional air quality model RAMS-CMAQ. *Atmos. Environ.* 214.
- Liu, F., Zhang, Q., vander A, R.J., Zheng, B., Tong, D., Yan, L., Zheng, Y.X., He, K.B., 2016. Recent reduction in NO_x emissions over China: synthesis of satellite observations and emission inventories. *Environ. Res. Lett.* 11.
- Liu, H.J., Wu, B.B., Liu, S.H., Shao, P.Y., Liu, X.Y., Zhu, C.Y., Wang, Y., Wu, Y.M., Xue, Y. F., Gao, J.J., Hao, Y., Tian, H.Z., 2018a. A regional high-resolution emission inventory of primary air pollutants in 2012 for Beijing and the surrounding five provinces of North China. *Atmos. Environ.* 181, 20–33.
- Liu, S.H., Hua, S.B., Wang, K., Qiu, P.P., Liu, H.J., Wu, B.B., Shao, P.Y., Liu, X.Y., Wu, Y. M., Xue, Y.F., Hao, Y., Tian, H.Z., 2018b. Spatial-temporal variation characteristics of air pollution in Henan of China: localized emission inventory, WRF/Chem simulations and potential source contribution analysis. *Sci. Total Environ.* 624, 396–406.
- Liu, S.H., Zhu, C.Y., Tian, H.Z., Wang, Y.X., Zhang, K., Wu, B.B., Liu, X.Y., Hao, Y., Liu, W., Bai, X.X., Lin, S.M., Wu, Y.M., Shao, P.Y., Liu, H.J., 2019. Spatiotemporal variations of ambient concentrations of trace elements in a highly polluted region of China. *J. Geophys. Res. Atmos.* 124, 4186–4202.
- Liu, X.Y., Bai, X.X., Tian, H.Z., Wang, K., Hua, S.B., Liu, H.J., Liu, S.H., Wu, B.B., Wu, Y. M., Liu, W., Luo, L.N., Wang, Y.X., Hao, J.M., Lin, S.M., Zhao, S., Zhang, K., 2020. Fine particulate matter pollution in North China: seasonal-spatial variations, source apportionment, sector and regional transport contributions. *Environ. Res.* 184, 109368.
- Lu, Y.L., Wang, Y., Zhang, W., Hubacek, K., Bi, F.F., Zuo, J., Jiang, H.Q., Zhang, Z.K., Feng, K.S., Liu, Y., Xie, W.B., 2019. Provincial air pollution responsibility and environmental tax of China based on interregional linkage indicators. *J. Clean. Prod.* 235, 337–347.
- Ma, Q., Cai, S.Y., Wang, S.X., Zhao, B., Martin, R.V., Brauer, M., Cohen, A., Jiang, J.K., Zhou, W., Hao, J.M., Frostad, J., Forouzanfar, M.H., Burnett, R.T., 2017. Impacts of coal burning on ambient PM_{2.5} pollution in China. *Atmos. Chem. Phys.* 17, 4477–4491.
- Ministry of Ecological and Environmental Protection of China and General Administration of Quality Supervision and Inspection Quarantine, 2012. Ambient air quality standard (GB 3095-2012). www.chinacsrmep.org/CSRTTool_Show_EN.asp?ID=285.
- National Bureau of Statistics of China, 2017. Statistical Communiqué of the People's Republic of China on the 2017 National Economic and Social Development.
- Nenes, A., Pandis, S.N., Pilinis, C., 1998. ISORROPIA: a new thermodynamic equilibrium model for multiphase multicomponent inorganic aerosols. *Aquat. Geochem.* 4, 123–152.
- Pleim, J.E., 2006. A combined local and nonlocal closure model for the atmospheric boundary layer. Part II: application and evaluation in a mesoscale meteorological model. *J. Appl. Meteorol. Climatol.* 46, 1396–1409.
- Pleim, J.E., 2007. A combined local and nonlocal closure model for the atmospheric boundary layer. Part I: model description and testing. *J. Appl. Meteorol. Climatol.* 46, 1383–1395.
- Pleim, J.E., Xiu, A.J., 1994. Development and testing of a surface flux and planetary boundary layer model for application in mesoscale models. *J. Appl. Meteorol.* 34, 16–32.
- Qi, J., Zheng, B., Li, M., Yu, F., Chen, C.C., Liu, F., Zhou, X.F., Yuan, J., Zhang, Q., He, K. B., 2017. A high-resolution air pollutants emission inventory in 2013 for the Beijing-Tianjin-Hebei region, China. *Atmos. Environ.* 170, 156–168.
- Skamarock, W.C., Klemp, J., Dudhia, J., Gill, D.O., Barker, D., Wang, W., Powers, J.G., 2008. A Description of the Advanced Research WRF Version 3, vol. 27, pp. 3–27.
- Streets, D.G., Bond, T.C., Carmichael, G.R., Fernandes, S.D., Yarber, K.F., 2003. An inventory of gaseous and primary aerosol emissions in Asia in the year 2000. *J. Geophys. Res. Atmos.* 108.
- Streets, D.G., Fu, J.S., Jang, C.J., Hao, J.M., He, K.B., Tang, X.Y., Zhang, Y.H., Wang, Z.F., Li, Z.P., Zhang, Q., Wang, L.T., Wang, B.Y., Yu, C., 2007. Air quality during the 2008 Beijing Olympic games. *Atmos. Environ.* 41, 480–492.
- Tan, J.N., Zhang, Y., Ma, W.C., Yu, Q., Wang, Q., Fu, Q.Y., Zhou, B., Chen, J.M., Chen, L. M., 2017. Evaluation and potential improvements of WRF/CMAQ in simulating multi-levels air pollution in megacity Shanghai, China. *Stoch. Environ. Res. Risk Assess.* 31, 2513–2526.
- The People's Government of Shanxi Province, 2015. Air pollution prevention and control action plan in Shanxi in 2015. <http://www.shanxi.gov.cn/>.
- US EPA, 2007. Guidance on the Use of Models and Other Analyses for Demonstrating Attainment of Air Quality Goals for Ozone, PM_{2.5}, and Regional Haze. Office of Air and Radiation/Office of Air Quality Planning and Standards, Research Triangle Park, NC.
- Valavanidis, A., Fiotakis, K., Vlachogianni, T., 2008. Airborne particulate matter and human health: toxicological assessment and importance of size and composition of particles for oxidative damage and carcinogenic mechanisms. *J. Environ. Sci. Heal. C.* 26, 339–362.
- Wang, S.X., Zhao, M., Xing, J., Wu, Y., Zhou, Y., Lei, Y., He, K.B., Fu, L.X., Hao, J.M., 2010. Quantifying the air pollutants emission reduction during the 2008 Olympic games in Beijing. *Environ. Sci. Technol.* 44, 2490–2496.
- Wang, L.T., Xu, J., Yang, J., Zhao, X.J., Wei, W., Cheng, D.D., Pan, X.M., Su, J., 2012. Understanding haze pollution over the southern Hebei area of China using the CMAQ model. *Atmos. Environ.* 56, 69–79.
- Wang, L.T., Wei, Z., Yang, J., Zhang, Y., Zhang, F.F., Su, J., Meng, C.C., Zhang, Q., 2014. The 2013 severe haze over southern Hebei, China: model evaluation, source apportionment, and policy implications. *Atmos. Chem. Phys.* 14, 3151–3173.
- Wang, J.K., Xu, J., He, Y.J., Chen, Y.B., Meng, F., 2016. Long range transport of nitrate in the low atmosphere over Northeast Asia. *Atmos. Environ.* 144, 315–324.
- Wang, J.D., Zhao, B., Wang, S.X., Yang, F.M., Xing, J., Morawska, L., Ding, A.J., Kulmala, M., Kerminen, V.M., Kujansuu, J., Wang, Z.F., Ding, D., Zhang, X.Y., Wang, H.B., Tian, M., Petaja, T., Jiang, J.K., Hao, J.M., 2017a. Particulate matter pollution over China and the effects of control policies. *Sci. Total Environ.* 584–585, 426–447.
- Wang, Y.J., Bao, S.W., Wang, S.X., Hu, Y.T., Shi, X., Wang, J.D., Zhao, B., Jiang, J.K., Zheng, M., Wu, M.H., Russell, A.G., Wang, Y.H., Hao, J.M., 2017b. Local and regional contributions to fine particulate matter in Beijing during heavy haze episodes. *Sci. Total Environ.* 580, 283–296.
- World Bank, 2016. World Bank and Institute for Health Metrics and Evaluation the Cost of Air Pollution: Strengthening the Economic Case for Action.
- Wu, W.J., Chang, X., Xing, J., Wang, S.X., Hao, J.M., 2017. Assessment of PM_{2.5} pollution mitigation due to emission reduction from main emission sources in the Beijing-Tianjin-Hebei region. *Environ. Sci.* 38, 867–875.
- Xiu, A.J., Pleim, J.E., 2000. Development of a land surface model. Part I: application in a mesoscale meteorological model. *J. Appl. Meteorol.* 40, 1.
- Xu, W.Z., He, C., Li, D.H., Zhao, F.S., Yan, Y., Proenv, J., 2013. A case study of aerosol characteristics during a haze episode over Beijing. *Procedia Environ. Sci.* 18, 404–411.
- Xu, Y.L., Xue, W.B., Lei, Y., Huang, Q., Zhao, Y., Cheng, S.Y., Ren, Z.H., Wang, J.N., 2020. Spatiotemporal variation in the impact of meteorological conditions on PM_{2.5} pollution in China from 2000 to 2017. *Atmos. Environ.* 223, 117215.
- Yan, Y., Peng, L., 2016. Emission inventory of anthropogenic VOCs and its contribution to ozone formation in Shanxi province. *Environ. Sci.* 37, 4086–4093.
- Yarwood, G., Rao, S., Yocke, M., Whitten, G., 2005. Updates to the Carbon Bond Chemical Mechanism: CB05 Final Report to the U.S. EPA, RT-0400675, p. 246.
- Yearbook of China Transportation & Communications, 2013. People's Communications Press, Beijing.

- Yearbook of China Transportation & Communications, 2016. People's Communications Press, Beijing.
- Yuan, M.C., Zu, B., Zhang, Q.X., Liu, P.H., Zhao, Y., 2018. Emission inventory and characteristics of anthropogenic air pollutant sources in Liaoning Province. *Acta Sci. Circumstantiae* 38, 1345–1357.
- Zhang, K., et al., 2017b. Gridded Emission Inventories and Spatial Distribution Characteristics of Major Air Pollutants in Lanzhou. Lanzhou University, China. Western China.
- Zhang, Y., Liu, P., Pun, B., Seigneur, C., 2006. A comprehensive performance evaluation of MM5-CMAQ for the Summer 1999 Southern Oxidants Study episode—Part I: evaluation protocols, databases, and meteorological predictions. *Atmos. Environ.* 40, 4825–4838.
- Zhang, Q., He, K.B., Huo, H., 2012a. Cleaning China's air. *Nature* 484, 161–162.
- Zhang, H.L., Li, J.Y., Qi, Y., Jian, Z.Y., Wu, D., Yuan, C., He, K.B., Jiang, J.K., 2012b. Source apportionment of PM_{2.5} nitrate and sulfate in China using a source-oriented chemical transport model. *Atmos. Environ.* 62, 228–242.
- Zhang, J.K., Sun, Y., Liu, Z.R., Ji, D.S., Hu, B., Liu, Q., Wang, Y.S., 2014. Characterization of submicron aerosols during a month of serious pollution in Beijing, 2013. *Atmos. Chem. Phys.* 14, 2887–2903.
- Zhang, Y.R., Zhang, H.L., Deng, J.J., Du, W.J., Hong, Y.W., Xu, L.L., Qiu, Y.Q., Hong, Z., Wu, X., Ma, Q.L., Yao, J., Chen, J.S., 2017a. Source regions and transport pathways of PM_{2.5} at a regional background site in East China. *Atmos. Environ.* 167, 202–211.
- Zhang, K.Q., Ma, Y.J., Xin, J.Y., Liu, Z.R., Ma, Y.N., Gao, D.D., Wu, J.S., Zhang, W.Y., Wang, Y.S., Shen, P.K., 2018. The aerosol optical properties and PM_{2.5} components over the world's largest industrial zone in Tangshan, North China. *Atmos. Res.* 201, 226–234.
- Zhao, B., Jiang, J.H., Gu, Y., Diner, D., Worden, J., Liou, K.N., Su, H., Xing, J., Garay, M., Huang, L., 2017a. Decadal-scale trends in regional aerosol particle properties and their linkage to emission changes. *Environ. Res. Lett.* 12.
- Zhao, B., Wu, W.J., Wang, S.X., Xing, J., Chang, X., Liou, K.N., Jiang, J.J., Gu, Y., Jang, Carey, Fu, J.S., 2017b. A modeling study of the nonlinear response of fine particles to air pollutant emissions in the Beijing-Tianjin-Hebei region. *Atmos. Chem. Phys.* 1–35.
- Zhao, B., Zheng, H.T., Wang, S.X., Smith, K.R., Lu, X., Aunan, K., Gu, Y., Wang, Y., Ding, D., Xing, J., Fu, X., Yang, X.D., Liou, K.N., Hao, J.M., 2018. Change in household fuels dominates the decrease in PM_{2.5} exposure and premature mortality in China in 2005–2015. *P. Natl. Acad. Sci. USA.* 115, 12401–12406.
- Zheng, B., Tong, D., Li, M., Liu, F., Hong, C.P., Geng, G.N., Li, H.Y., Li, X., Peng, L.Q., Qi, J., Yan, L., Zhang, Y.X., Zhao, H.Y., Zheng, Y.X., He, K.B., Zhang, Q., 2018. Trends in China's anthropogenic emissions since 2010 as the consequence of clean air actions. *Atmos. Chem. Phys.* 18, 14095–14111.